Published in final edited form as:
Chem Res Toxicol. 2009 April ; 22(4): 660–667. doi:10.1021/tx800478u.

Difference in Phototoxicity of Cyclodextrin Complexed Fullerene [(γ-CyD)$_2$/C_{60}] and Its Aggregated Derivatives toward Human Lens Epithelial Cells

Baozhong Zhao[†,‡], **Yu-Ying He**[†], **Colin F. Chignell**[†], **Jun-Jie Yin**[§], **Usha Andley**[‖], and **Joan E. Roberts**[*,‡,⊥]

Laboratory of Pharmacology, National Institute of Environmental Health Sciences, Research Triangle Park, North Carolina 27709, Center for Food Safety and Applied Nutrition, Food and Drug Administration, College Park, Maryland 20740, Department of Ophthalmology and Visual Science, Washington University School of Medicine, St. Louis, Missouri 63110, and Department of Natural Sciences, Fordham University, 113 West 60th Street, New York City, New York 10023

[†]National Institute of Environmental Health Sciences.

[§]Food and Drug Administration.

[‖]Washington University School of Medicine.

[⊥]Fordham University.

Abstract

The water-soluble fullerene derivative γ-cyclodextrin bicapped C_{60} [(γ-CyD)$_2$/C_{60}, CDF0] has several clinical applications, including use as a drug carrier to bypass the blood ocular barriers or a photosensitizer to treat tumors in photodynamic therapy. We have assessed the potential ocular toxicity of (γ-CyD)$_2$/C_{60} and its aggregated derivatives induced by UVA and visible light in vitro in human lens epithelial cells (HLE B-3). Cell viability using the MTS assay demonstrated that 2 μM (γ-CyD)$_2$/C_{60} was highly phototoxic to HLE B-3 cells with UVA irradiation, while no effect was observed in the presence of visible light or when maintained in the dark. In contrast, the aggregated derivative (CDF150) showed neither cytotoxicity nor any phototoxic effect even at 30 μM with either UVA or visible light irradiation. In lens cells treated with (γ-CyD)$_2$/C_{60}, phototoxicity was manifested as apoptosis. Singlet oxygen production measurement using the EPR/TEMP trapping technique determined that (γ-CyD)$_2$/C_{60} (CDF0) efficiently produced singlet oxygen. The rate of singlet oxygen production decreased with increased aggregation, with no production by the fully aggregated sample formed after 150 min of heating (CDF150). UVA irradiation of HLE B-3 in the presence of (γ-CyD)$_2$/C_{60} resulted in a significant rise in intracellular protein-derived peroxides. The singlet oxygen quenchers sodium azide and histidine each significantly protected lens cells against (γ-CyD)$_2$/C_{60} photodamage, but lutein and Trolox (vitamin E) did not. Clearly, singlet oxygen is an important intermediate in the phototoxicity of monomeric (γ-CyD)$_2$/fullerene. Our results also demonstrate that UVA-blocking sunglasses can limit the ocular phototoxicity of this nanomaterial, while nontoxic endogenous antioxidants like lutein or Trolox cannot provide adequate protection.

*To whom correspondence should be addressed. Tel: 212-636-6323. Fax: 212-636-7217. jroberts@fordham.edu..
‡Equal contribution by both authors.

Introduction

Nanomaterials have recently been manufactured on a large scale to be used in thousands of consumer goods and industrial products. However, because of their unique characteristics, interactions of nanomaterials with the environment in general and the human body in particular have the potential to damage human health. Because of their tiny size, nanoparticles can be absorbed deep into the lungs, and once in the bloodstream, some nanoparticles may cross the blood–brain barrier and blood–ocular barriers (1).

Water-soluble fullerenes have shown potential uses as drug carriers to bypass the brain and ocular barriers (2–4). Photoexcitation of fullerene derivatives efficiently produces an excited triplet state (5,6) and, through energy and electron transfer to molecular oxygen, produces both singlet molecular oxygen (7) and superoxide (8). We have previously found that γ-cyclodextrin bicapped C_{60} [$(\gamma\text{-CyD})_2/C_{60}$] is a very efficient singlet oxygen producer (9–11). Fullerenes have also exhibited anti-tumor and antiviral activities, including inhibition of HIV protease (12–15). Although the water-soluble fullerenes are not genotoxic (16), they are retained in the body for long periods, raising concerns about chronic toxic effects (17). The carboxylated water-soluble fullerene derivatives are not phototoxic to B lymphocytes (18), but the malonic acid derivatives of fullerenes are cytotoxic and phototoxic to both HeLa (19) and Jurkat cells (20). Other water-soluble hydroxylated fullerenes have been found to be cytotoxic to human dermal fibroblasts, human liver carcinoma cells (HepG2), and neuronal human astrocytes (21,22). We have previously found that hydroxylated fullerenes [fullerol, $C_{60}(OH)_{22–26}$] are both cytotoxic and phototoxic to human lens epithelial cells (HLE B-3)[1] (23).

The function of the human eye is to absorb light and use this light to control both vision and circadian rhythm (24). Ambient irradiation does not ordinarily damage the human lens because of its protective antioxidant system (25) and lens chromophores (e.g., 3-OH kynurenine glucoside) (26,27) that absorb light but do no harm. The cornea cuts off all light below 295 nm, but long wavelength UVB (295–315 nm) and ultraviolet A (UVA) (315–400 nm) are absorbed by the human lens (28). Phototoxic prescription drugs, diagnostic dyes, and over the counter herbal medications absorb light above 295 nm and produce reactive oxygen species

[1]Abbreviations:

DLS	dynamic light scattering
EPR	electron paramagnetic resonance
FBS	fetal bovine serum
HLE B-3	human lens epithelial cells
MEM	Eagle's Minimum Essential Medium
MTS	3-(4,5-dimethylthiazol-2-yl)-5-(3-carboxymethoxyphenyl)-2-(4-sulfophenyl)-2H-tetrazolium
PBS	phosphate buffered saline
ROS	reactive oxygen species
RT	room temperature
TCA	trichloroacetic acid
TEM	transmission electron microscopy
TEMP	2,2,6,6-tetramethyl-4-piperidone
TEMPO	2,2,6,6-tetramethyl-4-piperidone-N-oxyl radical
UVA	ultraviolet A (315–400 nm)

(ROS) that have the potential to initiate early cataracts and cause transient vision loss (29). Because (γ-CyD)$_2$/C_{60} has an absorbance maximum of 349 nm, it has the potential to cause lenticular damage when the human eye is exposed to UVA radiation.

In the studies presented here, we have assessed the difference in generation of singlet oxygen and ocular toxicity between cyclodextrin-complexed fullerene [(γ-CyD)$_2$/C_{60}] and its aggregated derivatives. We have determined that (γ-CyD)$_2$/C_{60} is highly phototoxic to HLE B-3 in the presence of UVA radiation. With aggregation, these compounds lose their phototoxicity. We have also demonstrated that UVA-blocking sunglasses should offer some protection against (γ-CyD)$_2$/C_{60} photodamage to the eye, while nontoxic endogenous antioxidants like lutein or Trolox (vitamin E) cannot provide adequate protection.

Materials and Methods

Chemicals

C_{60} (99.9%, sublimed), γ-cyclodextrin (γ-CyD, 99.0%), Eagle's minimum essential medium (MEM), gentamicin, L-glutamine, lutein, Trolox, histidine, and 2,2,6,6-tetramethyl-4-piperidone (TEMP) were all purchased from Sigma-Aldrich, Inc. (St. Louis, MO). Fetal bovine serum (FBS) was from Biofluids (Rockville, MD). *N*-Acetyl-L-cysteine was from Fluka (Milwaukee, WI). Trypsin-EDTA was from GIBCO Invitrogen Corporation (Carlsbad, CA).

Preparation of (γ-CyD)$_2$/C_{60} (CDF0) and Fullerene Aggregates (agg/C_{60}, CDF150) in Water Solutions

(γ-CyD)$_2$/C_{60} was prepared by the method of Yoshida et al. (30,31) with some modification. Briefly, a mixture of C_{60} (40.0 mg; 55.6 μmol) and γ-CyD (120.0 mg; 92.5 μmol) was stirred in a water/toluene (16/6 v/v) mixture at 118 °C for 48 h, and then, γ-CyD (60.0 mg; 46.3 μmol) was added twice more at 48 h intervals. After the mixture was cooled to room temperature (RT), the aqueous layer containing precipitated (γ-CyD)$_2$/C_{60} was vacuum filtered through a 0.22 μm nylon membrane. The purple crystals were washed with methanol to remove any free γ-CyD and dried in vacuo. To obtain a concentrated (γ-CyD)$_2$/C_{60} water solution, 3.5 mg of the solid was added to 5 mL of ultrapure water and heated at 85 °C for about 5 min until a clear solution formed. Then, the solution was filtered and sterilized by passing it through a 0.22 μm cellulose acetate membrane to remove the insoluble materials (C_{60} released from unstable complexes) and bacteria. The concentration of the solution was determined from its absorbance at 332 nm [log ε = 4.63 (31)]. This solution was prepared fresh before each use because the complex is unstable in water.

The (γ-CyD)$_2$/C_{60} water solution was unstable upon storage at RT; C_{60} molecules were released from the complex and formed a precipitate after 10 h (31). However, if the solution was heated to 85 °C for 150 min, it formed a transparent yellow solution that was relatively stable and could be stored for several days at RT without any observable precipitation. We have designated this preparation as agg/C_{60} (CDF150). The designation 150 refers to the heating time, as do the values 30, 60, 90, and 120 for the other intermediate samples: CDF30, CDF60, CDF90, and CDF120. With increased heating times, there is a concomitant increase in aggregation. The heating process was carried out in a sealed tube so that there was no solvent evaporation causing volume change and the concentration of C_{60} was equal to that of the original (γ-CyD)$_2$/C_{60} solution.

Characterization

All absorption spectra were recorded on an Agilent 8453 UV–visible spectrophotometer (Agilent Technologies, Inc., Santa Clara, CA). Transmission electron microscopy (TEM) images were taken on a Tecnai-12 Bio-Twin transmission electron microscope (FEI, The

Netherlands) operating at 80 kV. TEM grids were prepared by evaporating approximately 20 μL of water-soluble fullerene solution onto a 300 mesh carbon-coated copper grid. Dynamic light scattering (DLS) measurements of particle size were carried out using a light scattering Zetasizer Nano-S90 light scattering instrument (Malvern Instruments, Enigma Business Park, United Kingdom).

Cell Culture

An extended lifespan HLE B-3 line was used in these studies (32). HLE B-3 were cultured by isolating epithelium fragments from infant human lenses and from patients who underwent treatment for retinopathy of prematurity and by allowing epithelial cells to grow from explants. Cells were infected with an adenovirus, the 12-SV40 hybrid virus (Ad12-SV40), to increase their ability to propagate in culture.

Cells were grown in MEM (Sigma) containing 2 mM L-glutamine, 50 μg/mL gentamicin, and 20% FBS in an atmosphere of 5% CO_2/95% air at 37 °C. Cells were fed three times a week and, after attaining confluence, were passaged using trypsin (0.125%)–EDTA (0.5 mM).

In Vitro Cell Uptake of Fullerenes

The human lens cells were grown in 100 mm × 20 mm dishes to ~90% confluence at 37 °C in cell culture medium in an atmosphere of 95% air/5% CO_2. The medium was removed, and the cells were washed with Hank's balanced salt solution (HBBS) and then incubated with MEM (FBS-free) containing 20 μM fullerene. After incubation, the medium was removed, and the cells were washed twice with HBBS. The cells were then scraped, collected into a 15 mL tube, and spun down. The cells were diluted into 1 mL of water and transferred into a 1.5 mL tube. Each sample was sonicated using an Ultrasonic Homogenizer (Cole-Parmer, 4710 series) for 15 s and then centrifuged at 20000*g* for 10 min at 4 °C. The protein concentration was determined by using the BCA assay (Pierce, Rockford, CA). The fullerene concentration was estimated from the absorption spectra of the solution. The peak absorbance at 349 nm was compared to a standard curve prepared by addition of varying amounts of fullerenes in BSA solution (the concentration of BSA was adjusted to be approximately the same in each solution, with the protein concentration obtained by BCA assay). Note that this method does not discriminate between fullerenes bound to the cell membranes and those that are fully internalized.

Cell Viability

For photocytotoxicity tests, cells were exposed in the dark for 2 h at 37 °C to different fullerenes in HBSS. Control cells were treated with HBSS alone. After incubation, the medium was removed and replaced by sterile HBSS. Cells were then irradiated with UVA from four fluorescent PUVA lamps (Houvalite F20T12BL-HO; National Biological Co., Twinsburg, OH) or two cool white visible light lamps (Phillips F40 AX50, 5000 K Advantage); the UVA was filtered with a liquid filter to transmit only wavelengths above 400 nm (33). The fluencies were 15 and 5.4 J/cm^2, respectively, as measured with a YSI-Kettering model 65A Radiometer (Yellow Springs Instrument Co., Yellow Springs, OH). After exposure, the HBSS solution was removed and replaced with cell culture medium, and the cells were kept in the incubator overnight. The medium was removed, and the cells were washed with HBSS and then treated with 120 μL/well of HBSS containing the 3-(4,5-dimethylthiazol-2-yl)-5-(3-carboxymethoxyphenyl)-2-(4-sulfophenyl)-2H-tetrazolium (MTS) reagent (CellTiter 96 Aqueous Proliferation Assay; Promega Corp.). After incubation for 2 h at 37 °C, the absorbance at 492 nm was recorded using a microplate reader (Spectrafluor Plus, Tecan US, RTP, NC).

Measurement of Apoptotic and Necrotic Cells

Apoptotic and necrotic cells were quantitatively evaluated by flow cytometry (34,35). After treatment, the cells were harvested by trypsinization and collected by centrifugation at 300*g* for 5 min at RT. Cells were washed with cold phosphate-buffered saline (PBS) and stained with Annexin V-FITC and propidium iodide (PI) using a TACS Apoptosis Detection Kit according to the manufacturer's instructions (Trevigen, Gaithersburg, MD). Cells positive for PI, for Annexin V-FITC, or for both were quantified by flow cytometry using a Becton Dickinson FACSort (Becton Dickinson, Mountain View, CA). In the fluorescence dot plot histogram of Annexin V/PI-stained cells, the lower left quadrant shows normal viable cells, which are negative for both Annexin V and PI; the lower right quadrant shows early apoptotic cells, which are positive for Annexin V; the upper left quadrant shows necrotic cells, which are positive for PI, while the upper right quadrant shows late apoptotic cells, which are positive for both Annexin V and PI (34,35).

Electron Paramagnetic Resonance (EPR) Spectra

EPR spectra were recorded using a Varian E-109 Century line spectrometer (Varian Associates, Palo Alto, CA) operating at 9.78 GHz with 100 kHz modulation. All EPR spectra were recorded at RT in a quartz flat cell on a Bruker EMX EPR spectrometer equipped with a super high-Q cavity (Bruker, Billerica, MA). Spectra were recorded using an IBM-compatible computer interfaced with the spectrometer with the following instrument settings and conditions: 10 mW microwave power, 100 kHz modulation frequency, 1 G modulation amplitude, 20.5 ms time constant, 21 s scan time, and multiple scans of 80 G. Where indicated, samples were placed in a quartz flat cell and irradiated directly inside the microwave cavity of the spectrometer using a 1 kW Xe arc lamp. Radiation from the lamp was passed through a glass filter to remove wavelengths below 300 nm.

Measurement of Protein Peroxides

To measure protein peroxides, the human lens cells were suspended in HBBS, and 2 mL aliquots containing 3×10^6 cells were placed in individual wells of a six well plate (Becton Dickinson, Franklin Lakes, NJ). After the addition of 2 μM (γ-CyD)$_2$/C_{60} (CDF0) or 30 μM agg/C_{60} (CDF150), the cells were incubated at 37 °C for 2 h and then exposed to UVA radiation as described above for 20 min. Control cells either contained no fullerenes or were kept in the dark. Where indicated, sodium azide (10 mM) was present during treatment. Intracellular protein peroxides were assayed using a modified FOX assay as described by Wright et al. (36). Briefly, cells were collected from each well, and cold trichloroacetic acid (TCA) solution was added to give a 10% final concentration. The cells were then spun down, and the pellet was washed once with 1 mL of 10% TCA solution. The pellet was resuspended in 900 μL of 25 mM H_2SO_4, and 50 μL of a stock solution containing 5 mM $FeSO_4$ and 2 mM xylenol orange in 25 mM H_2SO_4 was added. The absorbance was measured at 560 nm after 30 min of incubation in the dark and compared to a standard curve prepared using H_2O_2.

Statistical Analysis

Data are expressed as means ± SEMs. The statistical significance was determined using ANOVA, followed by Bonferroni's *t* test using the StatView program (Abacus Concepts, Berkeley, CA). A value of $p < 0.05$ was considered statistically significant.

Results

Characterization of (γ-CyD)$_2$/C_{60} and Fullerene Aggregates

Fullerene (C_{60}) is known to be highly hydrophobic and insoluble in most polar solvents, especially water. We prepared nonaggregated water-soluble fullerene by complexation with

γ-CyD in the form of $(\gamma\text{-CyD})_2/C_{60}$, a noncovalent supermolecular complex. In water, it formed a clear lavender solution as shown in Figure 1A. This solution is not stable and when heated becomes a yellow aggregated solution. Thus, we simultaneously have two different types of fullerene water solution with the same C_{60} concentration. TEM images showed clearly that no aggregates were present before heating and uniformly dispersed aggregates were present after heating for 2.5 h (Figure 1B).

DLS measurements of particle size give a direct way to show the process of formation of fullerene aggregates. Figure 2 depicts the changes in particle size, which increased from 115.3 to 136.6 nm as the heating time increased from 30 to 150 min. We also recorded UV–visible absorption spectra of $(\gamma\text{-CyD})_2/C_{60}$ water solutions with different heating times. As shown in Figure 3, the absorption of $(\gamma\text{-CyD})_2/C_{60}$ (CDF0) in water showed three peaks (214, 260, and 332 nm). As the heating time increased, the intensities of the two peaks in the 200–300 nm region dramatically decreased and were slightly red-shifted, while the intensity of the 332 nm peak increased and was red-shifted. An additional broad absorption appeared in the 400–500 nm region. This broad absorption is characteristic of the aggregated state of crystalline C_{60} and is caused by close electronic interactions among adjacent C_{60} molecules (37–39).

Uptake of Fullerene by Lens Cells

To test the uptake of fullerene by lens cells, the fullerene solution was incubated with lens cells in serum-free MEM culture medium, and their uptake was measured after various exposure times. As shown in Figure 4, fullerene rapidly accumulated in the cells in a time-dependent manner, especially during the first 16 h; the uptake of agg/C_{60} (CDF150) was much higher than that of $(\gamma\text{-CyD})_2/C_{60}$.

Phototoxicity to Lens Cells

The phototoxicity of $(\gamma\text{-CyD})_2/C_{60}$ (CDF0) and agg/C_{60} (CDF30–150) toward HLE B-3 cells was measured using the MTS assay (which mainly measures the activity of mitochondrial dehydrogenases) (Figure 5). No obvious effect on viability was observed when lens cells were exposed to $(\gamma\text{-CyD})_2/C_{60}$ in the dark or in the presence of visible light (Figure 5A). However, in the presence of UVA irradiation, $(\gamma\text{-CyD})_2/C_{60}$ caused a concentration-dependent loss of mitochondrial activity. For agg/C_{60} (CDF150)-treated lens cells, no obvious effect on viability was observed even at fullerene concentrations up to 30 μM either in the dark or in the presence of UVA or visible light (Figure 5B). Figure 5C shows the phototoxicity toward lens cells of different fullerene water solutions with different heating times at the same concentration (2 μM); the phototoxicity of unaggregated fullerene was lost step by step with the formation of aggregates.

Analysis of $(\gamma\text{-CyD})_2/C_{60}$-Induced Apoptosis and Necrosis

We used flow cytometry to quantify necrotic and apoptotic HLE B-3 cells induced by $(\gamma\text{-CyD})_2/C_{60}$ and UVA irradiation. Early apoptosis is characterized by plasma membrane reorganization (34,35,40) and is detected by positive staining for Annexin V-FITC, while later stage apoptosis indicating DNA damage shows positive staining for both Annexin V and PI. We measured necrosis by determining the percentage of cells that was positive only for PI. In the absence of UVA irradiation, $(\gamma\text{-CyD})_2/C_{60}$ concentrations up to 2 μM had no effect on apoptosis or necrosis (Figure 6G). However, cells exposed to 0.25, 0.5, 1, and 2 μM $(\gamma\text{-CyD})_2/C_{60}$ plus UVA exhibited a concentration-dependent increase in apoptosis (Figure 6B–E,G). Pretreatment of cells with the singlet oxygen quencher NaN_3 showed significant protection against the $(\gamma\text{-CyD})_2/C_{60}$-induced apoptosis upon UVA exposure (Figure 6F,G). Exposure of HLE B-3 cells to UVA alone had no detectible effect on apoptosis or necrosis (Figure 6A).

Detection of Singlet Oxygen Generation by EPR

It has been previously reported that 2,2,6,6-tetramethyl-4-piperidone-N-oxyl radical (TEMPO), a nitroxide radical detectable by EPR spectra, is generated from TEMP and single oxygen (eq 1) (41)

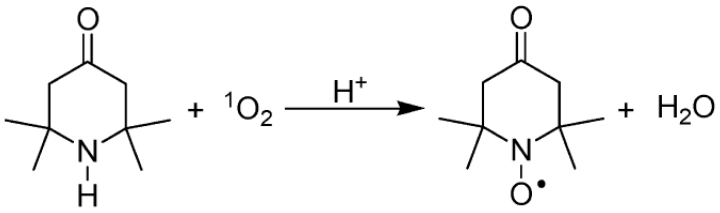

(1)

Here, irradiation of different fullerene samples (90 μM) containing 20 mM TEMP resulted in EPR spectra typical of nitroxide radicals: three lines with equal intensities (a_N = 16.0 G) (inset, Figure 7). The hyperfine splitting constant and *g* factor of the photosensitized oxidation product of TEMP were identical to those of commercial TEMPO. Figure 7 shows the EPR intensity of the TEMPO signal as a function of time of irradiation for different fullerene solutions. The (γ-CyD)$_2$/C_{60} (CDF0) solution showed the greatest rate of singlet oxygen production as measured by an increased TEMPO signal, while the rate of production decreased as aggregation was increased by heating. After 150 min of heating, there was no production of singlet oxygen. A control solution containing only TEMP exhibited no EPR signal increase. For the monomeric (γ-CyD)$_2$/C_{60} (CDF0), the addition of a singlet oxygen quencher, NaN_3, caused a dramatically reduced rate of increase in the EPR signal. These results are consistent with the above cell viability results, and they also suggest that the phototoxicity of (γ-CyD)$_2$/C_{60} is most likely mediated by a singlet oxygen (type II) mechanism.

Intracellular Formation of Protein Peroxides

To investigate the mechanism of (γ-CyD)$_2$/C_{60} phototoxicity, we used a modified FOX (36, 42) assay to measure the formation of protein peroxides in HLE B-3 cells loaded with fullerene derivatives. It is well known that singlet oxygen can oxidize many biomolecules, including membrane lipids, amino acids, cholesterol, and thiols. Furthermore, proteins are known to be the major intracellular targets for singlet oxygen due to their abundance and fast rates of reaction (36,43–45). As shown in Figure 8, negligible levels of protein peroxides were detected in control cells or in cells that had been preincubated with (γ-CyD)$_2$/C_{60} (CDF0) or agg/C_{60} (CDF150) and then kept in the dark. Exposure of the control cells to UVA irradiation generated 0.50 μM protein peroxides, which increased to 5.81 and 0.91 μM in the presence of 2 μM (γ-CyD)$_2$/C_{60} and agg/C_{60}, respectively. When the singlet oxygen quencher NaN_3 (10 mM) was present during irradiation, the protein peroxide level decreased to 0.35, 1.26, and 0.78 μM, respectively. These data indicate the presence of high levels of singlet oxygen-mediated protein peroxides in HLE B-3 cells exposed to (γ-CyD)$_2$/C_{60} and UVA radiation. They are also consistent with the observed singlet oxygen generation and cell viability results.

Inhibition of (γ-CyD)$_2$/C_{60} Phototoxicity to Lens Cells

To further determine the mechanism of (γ-CyD)$_2$/C_{60} phototoxicity and the possible involvement of reactive oxygen intermediates, we examined the effect of specific quenchers (lutein, NaN_3, the glutathione mimic *N*-acetyl-L-cysteine, the antioxidant Trolox, and histidine). We chose concentrations of (γ-CyD)$_2$/C_{60} (0.5 μM) that almost completely inhibited metabolic activity of the lens cells. As shown in Figure 9, histidine and the singlet oxygen quencher NaN_3 exhibited very effective protection against (γ-CyD)$_2$/C_{60} phototoxicity, while

N-acetyl-L-cysteine and Trolox were less effective. Surprisingly, lutein offered no obvious protection against (γ-CyD)$_2$/C_{60} phototoxicity.

Discussion

We report here a study of the ocular cytotoxicity and phototoxicity of (γ-CyD)$_2$/C_{60} and the influence of aggregation of fullerenes on these properties. The water-soluble (γ-CyD)$_2$/C_{60} is monomeric, but upon heating at 85 °C for up to 150 min, it becomes increasingly aggregated. We have confirmed this aggregation with both a TEM (Figure 1) and DLS (Figure 2). There is a change in the color (lavender to dark yellow, Figure 1A) and the absorbance spectra of these fullerene derivatives as they become increasingly aggregated (Figure 3).

The water-soluble fullerene derivative (γ-CyD)$_2$/C_{60} and its aggregates accumulate in the human lens cells. Because (γ-CyD)$_2$/C_{60} has very low fluorescence intensity, confocal microscopy could not be used to measure its uptake by the lens cells. Instead, uptake was confirmed by its absorbance at 349 nm (Figure 4).

Bicapped (γ-CyD)$_2$/C_{60} does not exhibit dark cytotoxicity and/or phototoxic effects on HLE B-3 in the presence of visible light. However, UVA irradiation in the presence of (γ-CyD)$_2$/C_{60} caused a concentration-dependent loss of mitochondrial activity and an increased rate of apoptosis. The levels of illumination that were chosen for the phototoxicity studies represent the amount of ambient UVA and visible light exposure one would expect on a bright, sunny day (46,47). UVA exposure included a cutoff filter to remove all radiation below 295 nm to mimic human corneal transmission (28). As the fullerene derivatives increased in aggregation, there was a decrease in phototoxic damage to the HLE B-3. These results are promising since fullerenes are more likely to be present in the environment in an aggregated form.

The lack of absorption of (γ-CyD)$_2$/C_{60} in the visible region could explain the absence of a phototoxic effect on HLE B-3 cells in the presence of visible light. Meanwhile, it is well-known that aggregation can deactivate the excited electronic states of photosensitizers and cause further loss of photoreactivity (48). The production of singlet oxygen as measured by EPR spin trapping showed that (γ-CyD)$_2$/C_{60} generated singlet oxygen efficiently, while such generation decreased as aggregation was increased by heating over time (Figure 7, from CDF0 to CDF150). This would explain the observed difference in phototoxicity between (γ-CyD)$_2$/C_{60} and its aggregates seen in Figure 5C. The uptake of agg/C_{60} (CDF150) by HLE B-3 cells is higher than that of (γ-CyD)$_2$/C_{60} (Figure 4), which excludes the possibility that the lower phototoxicity is due to reduced cellular uptake. Singlet oxygen is known to react directly with proteins and unsaturated lipids located in cell membranes to give the corresponding peroxides. The detection of protein peroxides as the major product during photoirradiation of HLE B-3 cells containing fullerenes and the quenching effect by azide strongly suggest that singlet oxygen is indeed generated inside the cells. Furthermore, 2 μM (γ-CyD)$_2$/C_{60} demonstrates a remarkably large increase in protein peroxides via $^1O_2$-mediated reactions, while 30 μM agg/C_{60} only shows a slight increase (Figure 8). Because the diffusion distance of singlet oxygen is very short [<70 nm (49)], this result also provides indirect evidence that photoreactive fullerene is taken up into cells. Apart from singlet oxygen (type II reaction), superoxide or hydroxyl radicals (type I reaction) may also play a minor role in the phototoxicity of (γ-CyD)$_2$/C_{60}, similar to our earlier findings, which reported the phototoxicity toward HaCaT cells (10).

On the other hand, bicapped (γ-CyD)$_2$/C_{60} fullerene derivatives, which are being considered for future medical use, have the potential to damage HLE B-3. In our previous studies (23), we found that another water-soluble fullerene derivative, fullerol, decreased metabolic activity in the HLE B-3 cells in the presence of 3.7 J cm^{-2} UVA and 5 μM fullerol, and this phototoxicity

could be partially prevented by the endogenous and nontoxic antioxidant lutein (50,51). Unfortunately, it appears that lutein does not provide any protection for the HLE B-3 against $(\gamma\text{-CyD})_2/C_{60}$ phototoxicity, nor did glutathione mimic *N*-acetyl-L-cysteine (52) or Trolox (water-soluble vitamin E). The singlet oxygen quenchers NaN_3 and histidine did decrease the phototoxic UVA damage caused by $(\gamma\text{-CyD})_2/C_{60}$. However, these quenchers are toxic and cannot be given as supplements to prevent damage. The decrease of phototoxic damage in the presence of the singlet oxygen quenchers NaN_3 and histidine did confirm that the phototoxic mechanism of damage of $(\gamma\text{-CyD})_2/C_{60}$ with UVA very likely involves singlet oxygen as one of the main ROS (type II mechanism).

Enhanced production of ROS within the lens of the eye and consequent oxidative damage to the lens proteins is thought to be a major mechanism leading to the onset of cataracts (29). Bicapped $(\gamma\text{-CyD})_2/C_{60}$ induced apoptosis in the human lens cells, and apoptosis has also been shown to lead to the development of cataracts (53). It is fortunate that $(\gamma\text{-CyD})_2/C_{60}$ primarily shows UVA phototoxicity and very little cytotoxicity or visible light phototoxicity because it is relatively easy to prevent UVA radiation from reaching the human lens. The use of UVA-blocking wrap-around sunglasses (54) will protect critical components of the lens against much of the phototoxic damage by $(\gamma\text{-CyD})_2/C_{60}$.

In conclusion, monomeric $(\gamma\text{-CyD})_2/C_{60}$ is highly phototoxic to HLE B-3 cells with UVA irradiation, while no effect was observed in the presence of visible light. No phototoxic effect was seen for its aggregated derivatives even at high concentrations, with either UVA or visible light exposure. UVA-blocking sunglasses should offer some protection against $(\gamma\text{-CyD})_2/C_{60}$ photodamage to the eye. Nontoxic endogenous antioxidants like lutein or Trolox (vitamin E) cannot provide adequate protection against $(\gamma\text{-CyD})_2/C_{60}$ UVA phototoxicity. Finally, our findings indicate that $(\gamma\text{-CyD})_2/C_{60}$ could potentially be used in photodynamic therapy to kill tumor cells because it produces singlet oxygen very efficiently. On the other hand, concern is also warranted about the use of $(\gamma\text{-CyD})_2/C_{60}$ and other fullerenes as a drug or drug carriers in human trials without further ocular toxicity studies.

Acknowledgments

This paper is dedicated to the memory of Dr. Colin F. Chignell. This research was supported by the Intramural Research Program of the NIH, National Institute of Environmental Health Sciences. We thank Dr. Ann Motten, NIEHS, for help in preparation of this manuscript and Dr. Carl Bortner and Maria Sifre for their assistance with flow cytometry measurements. This manuscript has been reviewed by the National Institutes of Environmental Health Sciences and approved for publication.

References

(1). Kreuter J. Application of nanoparticles for the delivery of drugs to the brain. Int. Congr. Ser 2005;1277:85–94.

(2). Calvo P, Sanchez A, Martinez J, Lopez MI, Calonge M, Pastor JC, Alonso MJ. Polyester nanocapsules as new topical ocular delivery systems for cyclosporin A. Pharm. Res 1996;13:311–315. [PubMed: 8932455]

(3). Da Ros T, Prato M. Medicinal chemistry with fullerenes and fullerene derivatives. Chem. Commun 1999:663–669.

(4). Dugan LL, Turetsky DM, Du C, Lobner D, Wheeler M, Almli CR, Shen CK, Luh TY, Choi DW, Lin TS. Carboxyfullerenes as neuroprotective agents. Proc. Natl. Acad. Sci. U.S.A 1997;94:9434–9439. [PubMed: 9256500]

(5). Arbogast JW, Darmanyan AP, Foote CS, Rubin Y, Diederich FN, Alvarez MM, Anz SJ, Whetten RL. Photophysical properties of C60. J. Phys. Chem 1991;95:11–12.

(6). Guldi DM, Prato M. Excited-state properties of C(60) fullerene derivatives. Acc. Chem. Res 2000;33:695–703. [PubMed: 11041834]

(7). Prat F, Stackow R, Bernstein R, Qian W, Rubin Y, Foote CS. Triplet state properties and singlet oxygen generation in homologous series of functionalised fullerene derivatives. J. Phys. Chem 1999;103:7230–7235.

(8). Yamakoshi Y, Umezawa N, Ryu A, Arakane K, Miyata N, Goda Y, Masumizu T, Nagano T. Active oxygen species generated from photoexcited fullerene (C60) as potential medicines: O^{2-}* versus $^1O_2$. J. Am. Chem. Soc 2003;125:12803–12809. [PubMed: 14558828]

(9). Zhao B, Bilski PJ, He YY, Feng L, Chignell CF. Photo-induced reactive oxygen species generation by different water-soluble fullerenes (C) and their cytotoxicity in human keratinocytes. Photochem. Photobiol 2008;84:1215–1223. [PubMed: 18399919]

(10). Zhao B, He YY, Bilski PJ, Chignell CF. Pristine (C60) and hydroxylated [C60(OH)24] fullerene phototoxicity towards HaCaT keratinocytes: Type I vs type II mechanisms. Chem. Res. Toxicol 2008;21:1056–1063. [PubMed: 18422350]

(11). Bilski P, Zhao BZ, Chignell CF. Singlet oxygen phosphorescence photosensitized in nano-aggregates of C-60 buck-minsterfullerene is insensitive to solvent and quenchers and strongly red-shifted indicating highly polarizable interior. Chem. Phys. Lett 2008;458:157–160.

(12). Bogdanovic G, Kojic V, Dordevic A, Canadanovic-Brunet J, Vojinovic-Miloradov M, Baltic VV. Modulating activity of fullerol C60(OH)22 on doxorubicin-induced cytotoxicity. Toxicol. in Vitro 2004;18:629–637. [PubMed: 15251181]

(13). Friedman DL, DeCamp R, Sijbesma G, Srdanov G, Wudl F, Kenyon GL. Inhibition of the HIV-1 protease by fullerene derivatives: Model building studies and experimental verification. J. Am. Chem. Soc 1993;115:6506–6509.

(14). Nakamura E, Isobe H. Functionalized fullerenes in water. The first 10 years of their chemistry, biology, and nanoscience. Acc. Chem. Res 2003;36:807–815. [PubMed: 14622027]

(15). Schinazi RF, Sijbesma R, Srdanov G, Hill CL, Wudl F. Synthesis and virucidal activity of a water-soluble, configurationally stable, derivatized C60 fullerene. Antimicrob. Agents Chemother 1993;37:1707–1710. [PubMed: 8215289]

(16). Zakharenko LP, Zakharov IK, Vasiunina EA, Karamysheva TV, Danilenko AM, Nikiforov AA. Determination of the genotoxicity of fullerene C60 and fullerol using the method of somatic mosaics on cells of Drosophila melanogaster wing and SOS-chromotest. Genetika 1997;33:405–409. [PubMed: 9244774]

(17). Yamago S, Tokuyama H, Nakamura E, Kikuchi K, Kananishi S, Sueki K, Nakahara H, Enomoto S, Ambe F. In vivo biological behavior of a water-miscible fullerene: 14C labeling, absorption, distribution, excretion and acute toxicity. Chem. Biol 1995;2:385–389. [PubMed: 9383440]

(18). Irie K, Nakamura Y, Ohigashi H, Tokuyama H, Yamago S, Nakamura E. Photocytotoxicity of water-soluble fullerene derivatives. Biosci., Biotechnol., Biochem 1996;60:1359–1361. [PubMed: 8987557]

(19). Yang XL, Fan CH, Zhu HS. Photo-induced cytotoxicity of malonic acid [C(60)]fullerene derivatives and its mechanism. Toxicol. in Vitro 2002;16:41–46. [PubMed: 11812638]

(20). Rancan F, Rosan S, Boehm F, Cantrell A, Brellreich M, Schoenberger H, Hirsch A, Moussa F. Cytotoxicity and photocytotoxicity of a dendritic C(60) mono-adduct and a malonic acid C(60) tris-adduct on Jurkat cells. J. Photochem. Photobiol., B 2002;67:157–162. [PubMed: 12167314]

(21). Sayes CM, Fortner JD, Guo W, Lyon D, Boyd AM, Ausman KD, Tao YJ, Sitharaman B, Wilson LJ, Hughes JB, West JL, Colvin VL. The differential cytotoxicity of water-soluble fullerenes. Nano Lett 2004;4:1881–1887.

(22). Sayes CM, Gobin AM, Ausman KD, Mendez J, West JL, Colvin VL. Nano-C60 cytotoxicity is due to lipid peroxidation. Biomaterials 2005;26:7587–7595. [PubMed: 16005959]

(23). Roberts JE, Wielgus AR, Boyes WK, Andley U, Chignell CF. Phototoxicity and cytotoxicity of fullerol in human lens epithelial cells. Toxicol. Appl. Pharmacol 2008;228:49–58. [PubMed: 18234258]

(24). Roberts JE. Update on the positive effects of light in humans. Photochem. Photobiol 2005;81:490–492. [PubMed: 15656701]

(25). Andley, UP. Ocular Lens Photobiology. Valdenmar Publishing Company; Overland Park, KS: 2001.

(26). Balasubramanian D. Ultraviolet radiation and cataract. J. Ocul. Pharmacol. Ther 2000;16:285–297. [PubMed: 10872925]

(27). Dillon J. The photophysics and photobiology of the eye. J. Photochem. Photobiol., B 1991;10:23–40. [PubMed: 1955945]

(28). Barker FM, Brainard GC, Dayhaw-Barker P. Transmission of the human lens as a function of age. Invest. Ophthalmol. Vis. Sci 1991;32S:1083.

(29). Roberts JE. Screening for ocular phototoxicity. Int. J. Toxicol 2002;21:491–500. [PubMed: 12537645]

(30). Nishibayashi Y, Saito M, Uemura S, Takekuma S, Takekuma H, Yoshida Z. Buckminsterfullereness—A non-metal system for nitrogen fixation. Nature 2004;428:279–280. [PubMed: 15029186]

(31). Yoshida ZI, Takekuma H, Takekuma SI, Matsubara Y. Molecular recognition of C-60 with gamma-cyclodextrin. Angew. Chem., Int. Ed 1994;33:1597–1599.

(32). Andley UP, Rhim JS, Chylack LT Jr. Fleming TP. Propagation and immortalization of human lens epithelial cells in culture. Invest. Ophthalmol. Vis. Sci 1994;35:3094–3102. [PubMed: 8206728]

(33). Wielgus AR, Chignell C, Miller DS, Van Houten B, Meyer J, Hu DN, Roberts JE. Phototoxicity in human retinal epithelial cells promoted by hypericin, a component of St. John's Wort. Photochem. Photobiol 2007;83:706–713. [PubMed: 17576381]

(34). Martin SJ, Reutelingsperger CP, McGahon AJ, Rader JA, van Schie RC, LaFace DM, Green DR. Early redistribution of plasma membrane phosphatidylserine is a general feature of apoptosis regardless of the initiating stimulus: inhibition by overexpression of Bcl-2 and Abl. J. Exp. Med 1995;182:1545–1556. [PubMed: 7595224]

(35). Reno F, Burattini S, Rossi S, Luchetti F, Columbaro M, Santi S, Papa S, Falcieri E. Phospholipid rearrangement of apoptotic membrane does not depend on nuclear activity. Histochem. Cell Biol 1998;110:467–476. [PubMed: 9826126]

(36). Wright A, Hawkins CL, Davies MJ. Photo-oxidation of cells generates long-lived intracellular protein peroxides. Free Radical Biol. Med 2003;34:637–647. [PubMed: 12633741]

(37). Bensasson RV, Bienvenue E, Dellinger M, Leach S, Seta P. C60 in model biological-systemss—A visible-UV absorption study of solvent-dependent parameters and solute aggregation. J. Phys. Chem 1994;98:3492–3500.

(38). Fortner JD, Lyon DY, Sayes CM, Boyd AM, Falkner JC, Hotze EM, Alemany LB, Tao YJ, Guo W, Ausman KD, Colvin VL, Hughes JB. C-60 in water: Nanocrystal formation and microbial response. Environ. Sci. Technol 2005;39:4307–4316. [PubMed: 15984814]

(39). Hungerbuhler H, Guldi DM, Asmus KD. Incorporation of C-60 into artificial lipid-membranes. J. Am. Chem. Soc 1993;115:3386–3387.

(40). Singh N. A simple method for accurate estimation of apoptotic cells. Exp. Cell Res 2000;256:328–337. [PubMed: 10739681]

(41). Lion Y, Delmelle M, van de Vorst A. New method of detecting singlet oxygen production. Nature 1976;263:442–443. [PubMed: 972689]

(42). Gay C, Collins J, Gebicki JM. Hydroperoxide assay with the ferric-xylenol orange complex. Anal. Biochem 1999;273:149–155. [PubMed: 10469484]

(43). Davies MJ, Hawkins C, Wright A. Singlet oxygen-mediated formation of protein peroxides within cells. Free Radical Biol. Med 2002;33:S420–S420.

(44). Kochevar IE, Bouvier J, Lynch M, Lin CW. Influence of dye and protein location on photosensitization of the plasma-membrane. Biochim. Biophys. Acta, Biomembr 1994;1196:172–180.

(45). Wilkinson F, Helman WP, Ross AB. Rate constants for the decay and reactions of the lowest electronically excited singlet-state of molecular-oxygen in solution—An expanded and revised compilation. J. Phys. Chem. Ref. Data 1995;24:663–1021.

(46). Diffey BL. The calculation of the spectral distribution of natural ultraviolet radiation under clear day conditions. Phys. Med. Biol 1977;22:309–316. [PubMed: 857265]

(47). Sliney DH. How light reaches the eye and its components. Int. J. Toxicol 2002;21:501–509. [PubMed: 12537646]

(48). Oba T. Photosensitizer nanoparticles for photodynamic therapy. Curr. Bioact. Compd 2007;3:239–251.

(49). Moan J. On the diffusion length of singlet oxygen in cells and tissues. J. Photochem. Photobiol., B 1990;6:343–347.

(50). Hankinson SE, Stampfer MJ, Seddon JM, Colditz GA, Rosner B, Speizer FE, Willett WC. Nutrient intake and cataract extraction in women: a prospective study. Br. Med. J 1992;305:335–339. [PubMed: 1392884]

(51). Yeum KJ, Taylor A, Tang G, Russell RM. Measurement of carotenoids, retinoids, and tocopherols in human lenses. Invest. Ophthalmol. Vis. Sci 1995;36:2756–2761. [PubMed: 7499098]

(52). Busch EM, Gorgels TG, Roberts JE, van Norren D. The effects of two stereoisomers of N-acetylcysteine on photochemical damage by UVA and blue light in rat retina. Photochem. Photobiol 1999;70:353–358. [PubMed: 10483364]

(53). Okamurai NIY, Shibata M-A, Ikeda T, Otsuki Y. Fas-mediated apoptosis in human lens epithelial cells of cataracts associated with diabetic retinopathy. Med. Electron Microsc 2002;35:234–241. [PubMed: 12658358]

(54). Sliney DH. Photoprotection of the eyes—UV radiation and sunglasses. J. Photochem. Photobiol., B 2001;64:166–175. [PubMed: 11744403]

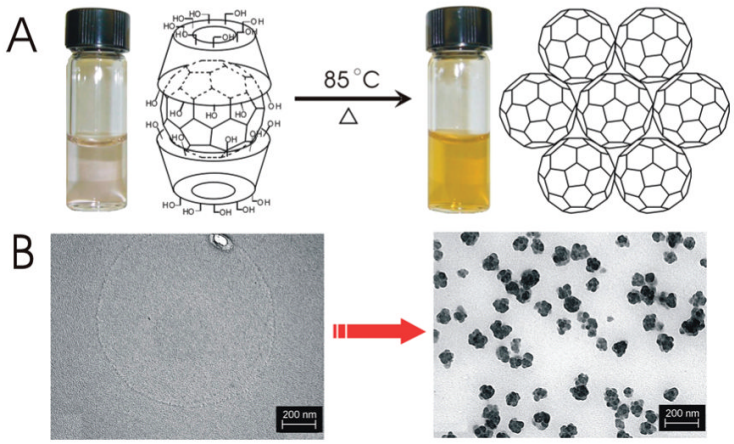

Figure 1.

(A) Preparation and visual images of (γ-CyD)$_2$/C_{60} and fullerene aggregates (agg/C_{60}) in aqueous solution. (B) TEM images of (γ-CyD)$_2$/C_{60} (CDF0) and agg/C_{60} (CDF150).

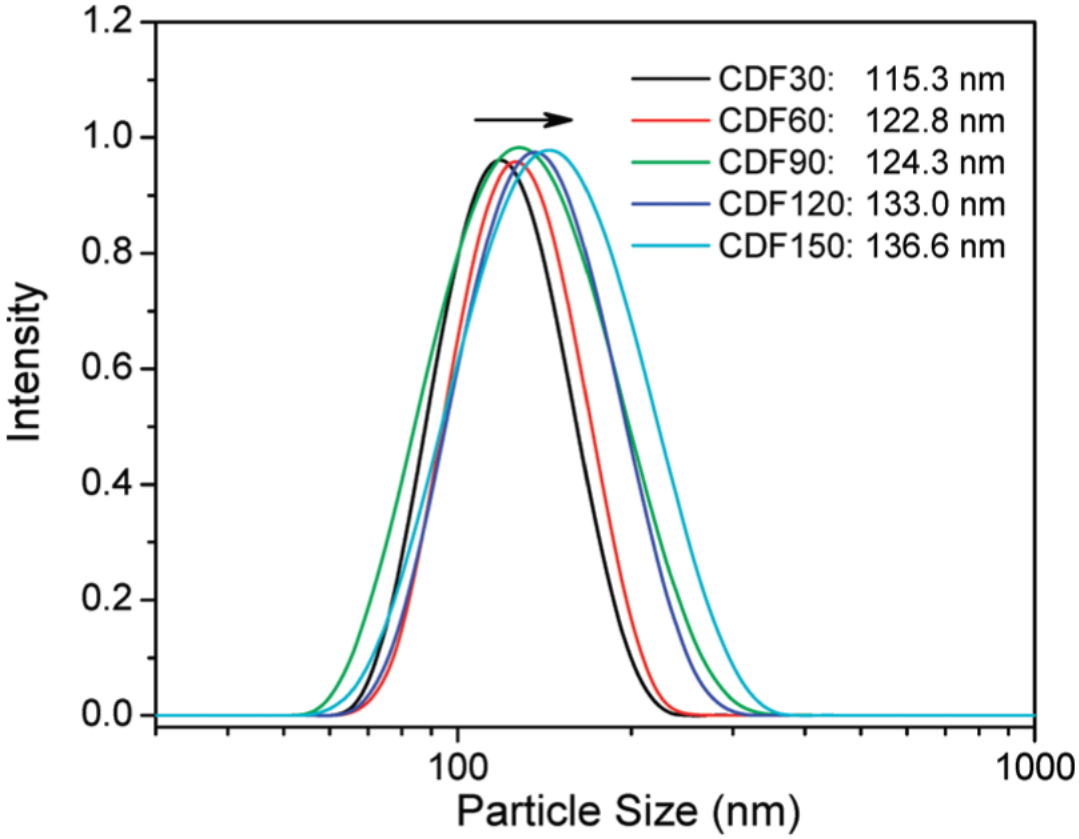

Figure 2.
DLS determination of particle size and distribution of 10 μM fullerene water solution with different heating times. The *Z*-average sizes from CDF30 to CDF150 are 115.3, 122.8, 124.3, 133.0, and 136.6 nm, respectively.

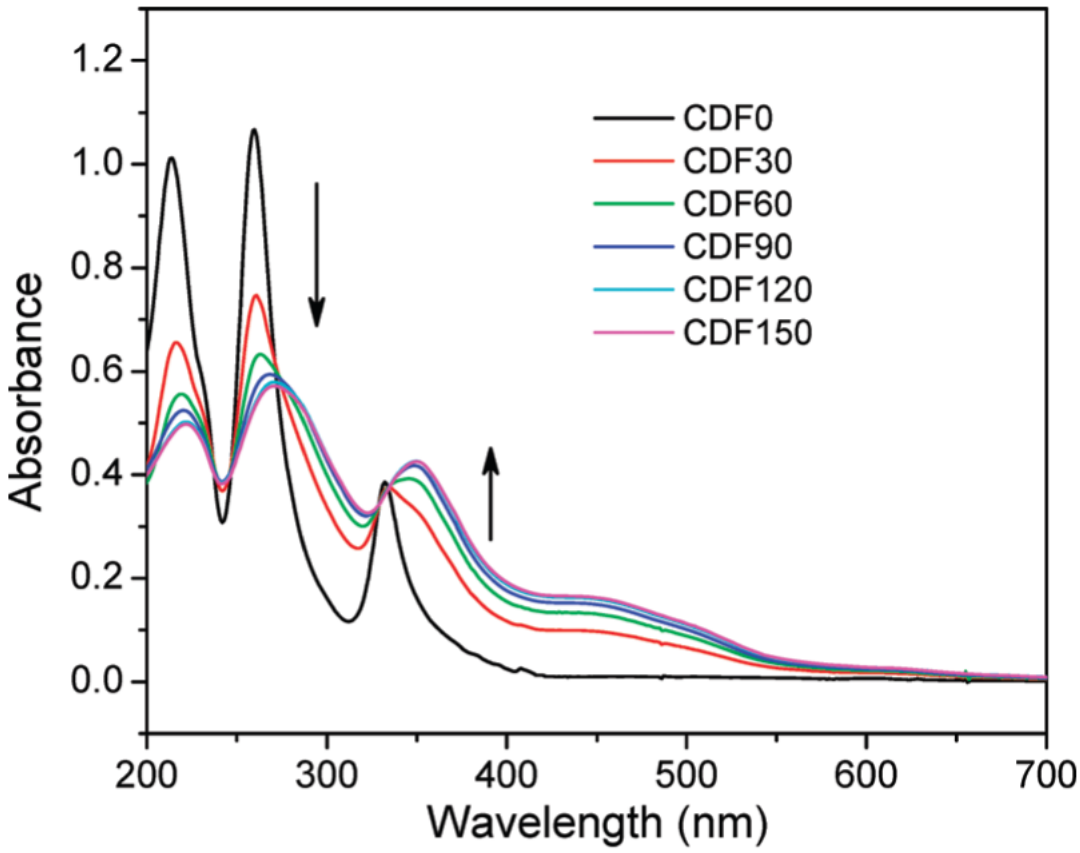

Figure 3.
Changes in UV–vis absorption spectra of 10 μM fullerene water solution with different heating times at 85 °C. Spectra from CDF0 to CDF150 correspond to heating times of 0, 30, 60, 90, 120, and 150 min.

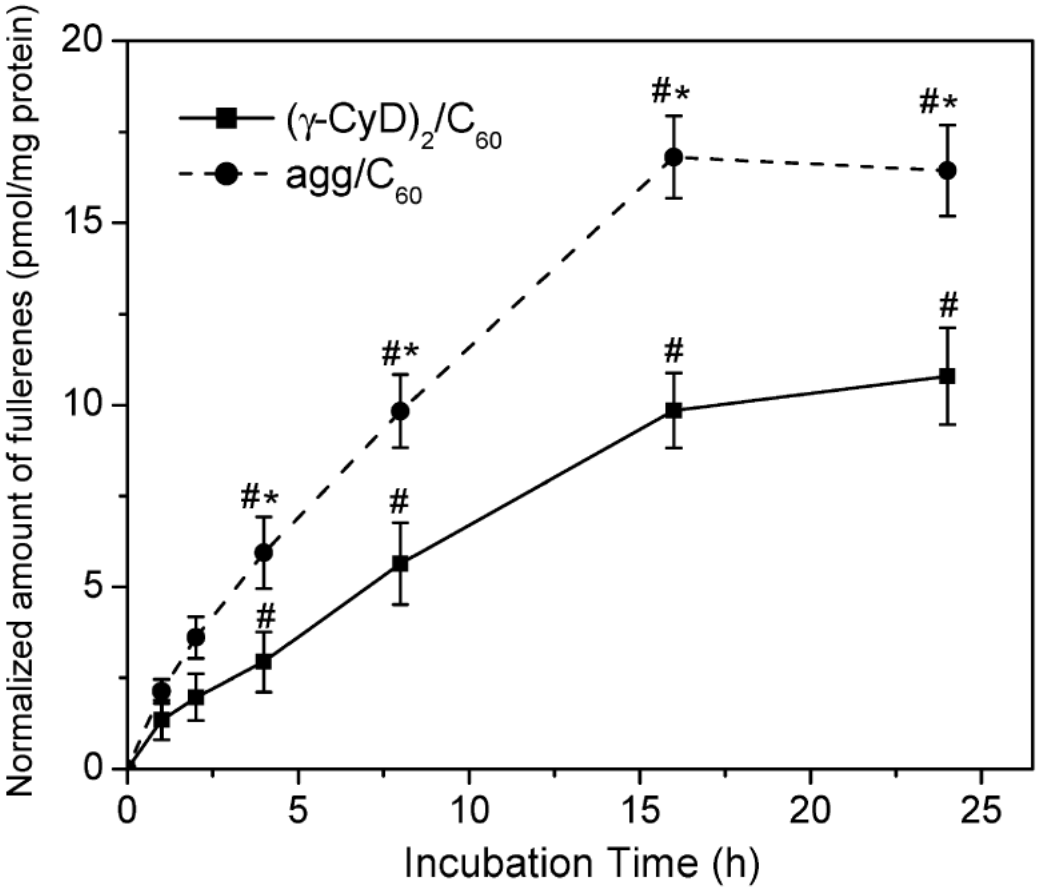

Figure 4.

Uptake of $(\gamma\text{-CyD})_2/C_{60}$ (CDF0) and agg/C_{60} (CDF150) by HLE B-3 cells. The cells were incubated in the dark in MEM containing 20 μM $(\gamma\text{-CyD})_2/C_{60}$ or agg/C_{60}. The amount of fullerenes in cells was determined spectrophotometrically and normalized to the concentration of protein. Results were presented as the means ± SEMs from three independent experiments in duplicate. $^{\#}p < 0.05$ as compared with cells without fullerene treatment. $^{*}p < 0.05$ as compared with corresponding agg/C_{60}-treated cells.

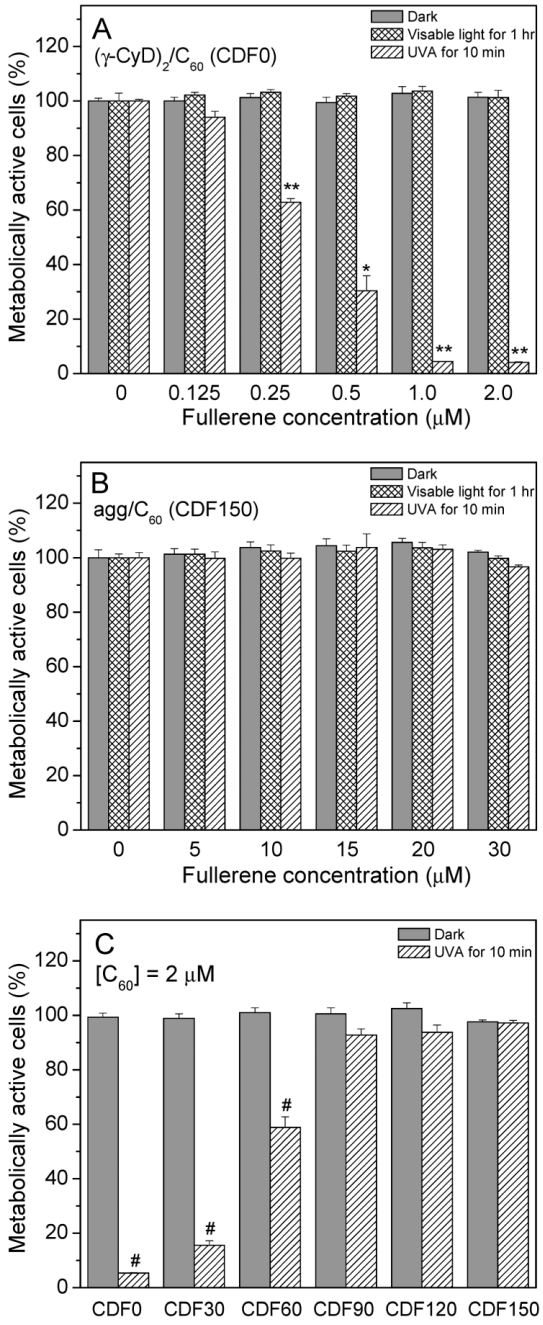

Figure 5.

Effect of different concentrations of (A) $(\gamma\text{-CyD})_2/C_{60}$ (CDF0) and (B) agg/C_{60} (CDF150) on the viability of HLE B-3 cells irradiated with UVA (15 J/cm^2) and cool white light (5.4 J/cm^2) as measured by the MTS assay (see the Materials and Methods). (C) Effect of 2 μM fullerene water solutions as a function of heating time on the viability of HLE B-3 cells irradiated with UVA. Results were presented as the means ± SEMs from three independent experiments in quadruplicate. $^{**}p < 0.01$ and $^{*}p < 0.05$ as compared with cells without fullerene treated and in the dark. $^{\#}p < 0.01$ as compared with corresponding cells in the dark.

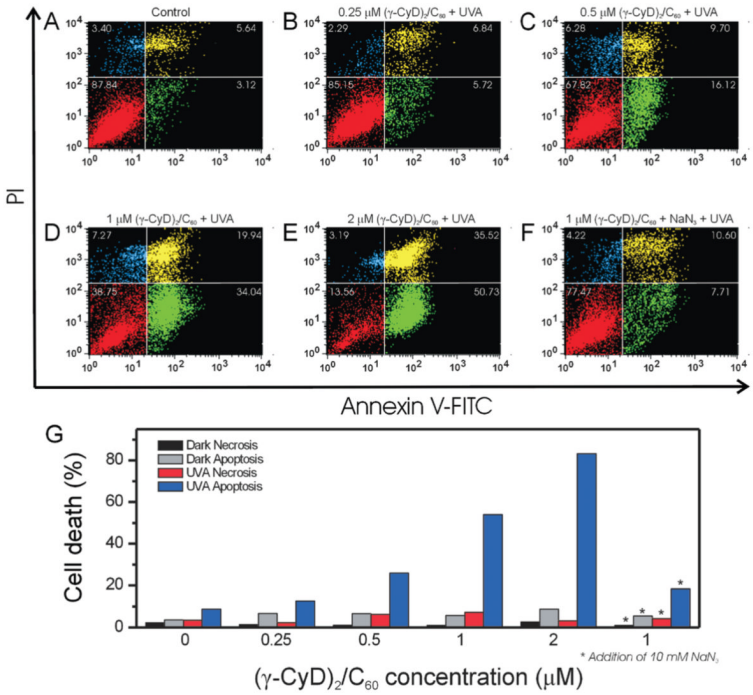

Figure 6.

(γ-CyD)$_2$/C$_{60}$-induced apoptotic and necrotic death in HLE B-3 cells with UVA irradiation. (A–E) Cells were seeded in plastic Petri dishes (60 cm^2) and pretreated with (γ-CyD)$_2$/C$_{60}$ at different concentrations in HBSS for 2 h and then exposed to UVA (10 min). After irradiation, the cells were incubated overnight in cell culture medium and then stained with Annexin V-FITC and PI. Apoptotic and necrotic cell death were determined with flow cytometry. For the NaN_3 protection assay (F), cells were incubated with 10 mM NaN_3 during the incubation period as well as the irradiation period. (G) Graphs illustrating UVA irradiation-induced (γ-CyD)$_2$/C$_{60}$ dose-dependent apoptosis and necrosis and the protection effect by NaN_3.

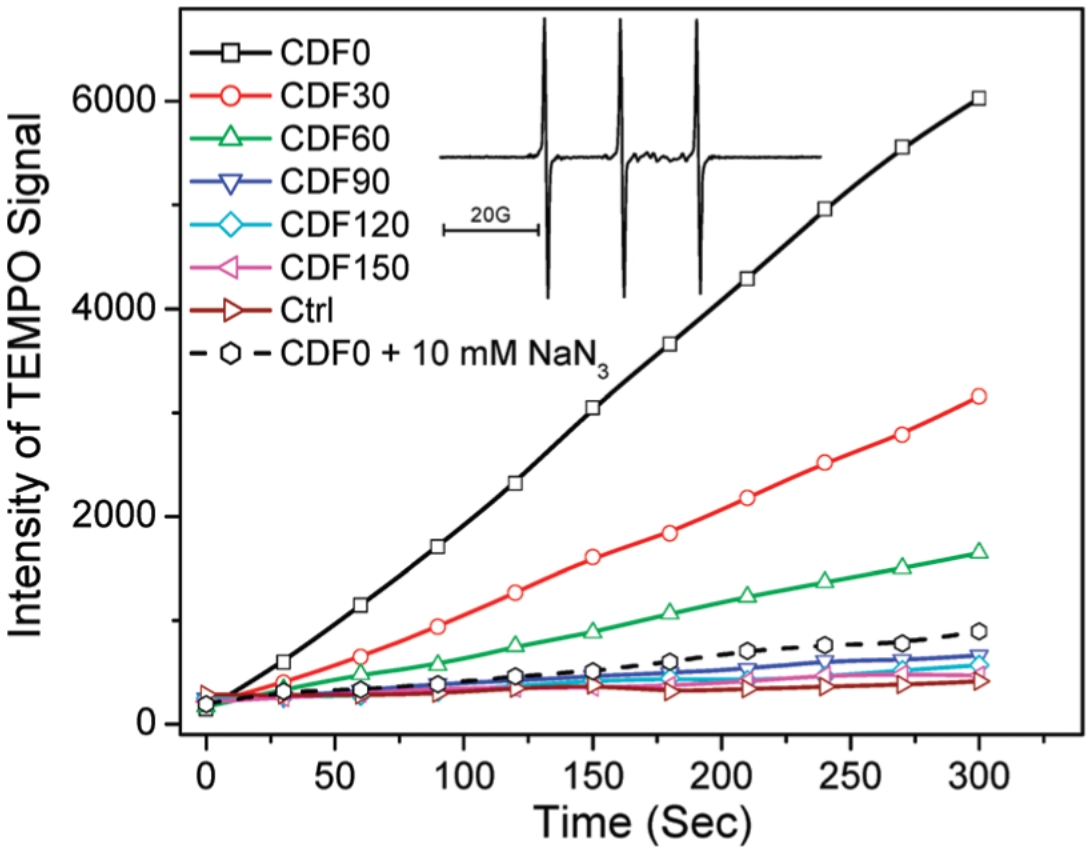

Figure 7.

Intensity of TEMPO signal as a function of time during irradiation of different fullerene water solutions. The TEMPO signal was measured with the EPR technique for solutions containing 20 mM TEMP and (i–vi) unaggregated and aggregated fullerene samples in water containing 90 μM C_{60}, (vii) H_2O only as control, and (viii) 90 μM (γ-CyD)$_2$/C_{60} (CDF0) in addition to 10 mM NaN_3 in water. Measurements were made for 21 s periods, with 9 s intervals between each measurement. During the measurements, the samples were exposed to irradiation ($\lambda > 300$ nm). Inset: EPR signal of TEMPO (a_N = 16.0 G). Instrumental settings: microwave power, 10 mW; modulation frequency, 100 kHz; modulation amplitude, 1 G; time constant, 20.5 ms; 21.0 s scan time; and scan range, 80 G.

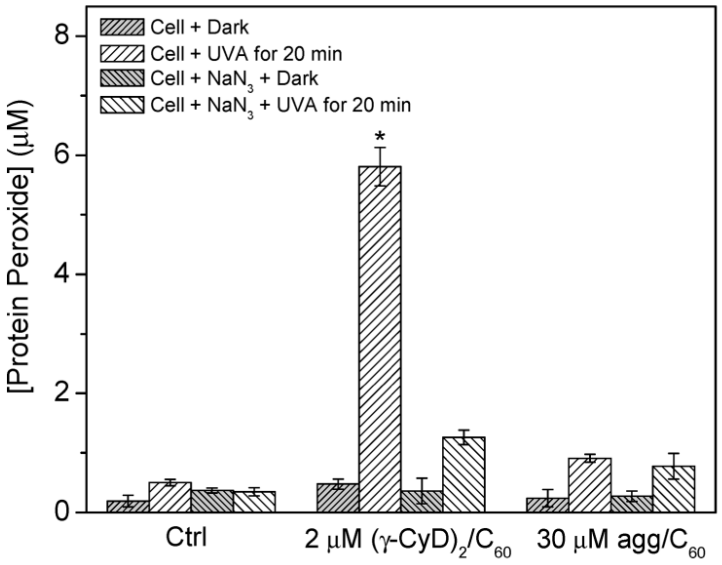

Figure 8.

Effect of (γ-CyD)$_2$/C$_{60}$ (CDF0) and agg/C$_{60}$ (CDF150) exposure on the formation of protein peroxides during illumination of HLE B-3 cells in the absence or presence of 10 mM sodium azide. Cells (1.5×10^6 cells mL^{-1}) were incubated with 2 μM (γ-CyD)$_2$/C$_{60}$ (CDF0) or 30 μM agg/C$_{60}$ (CDF150) for 2 h before illumination with UVA (30 J/cm^2) for 20 min. Results were presented as the means ± SEMs from three independent experiments in quadruplicate. *p < 0.05 as compared with corresponding control cells.

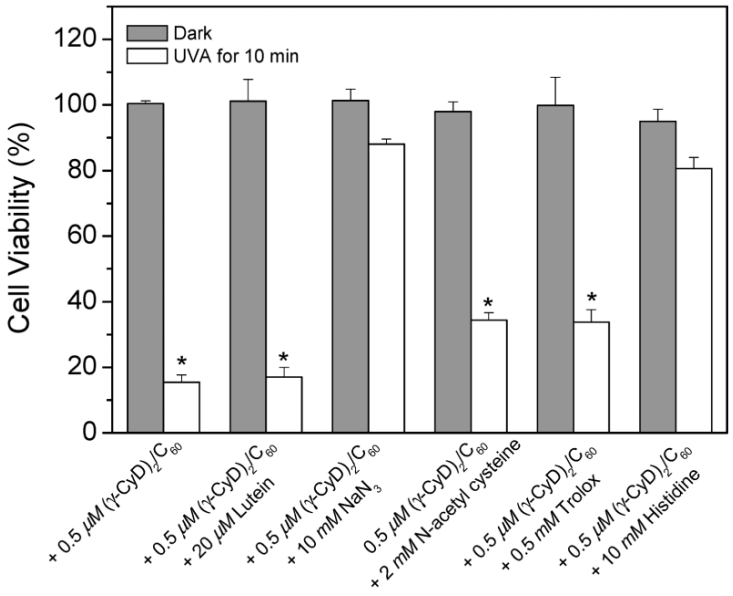

Figure 9.

Effect of lutein (20 μM), sodium azide (10 mM), *N*-acetyl cysteine (2 mM), Trolox (0.5 mM), and histidine (10 mM) on the photocytotoxicity of (γ-CyD)$_2$/C$_{60}$ toward HLE B-3 cells. For the inhibitory studies, antioxidants were used during the incubation period as well as the irradiation period (UVA, 15 J/cm^2). Results were presented as the means ± SEMs from three independent experiments in quadruplicate. *$p < 0.05$ as compared with corresponding (γ-CyD)$_2$/C$_{60}$-treated cells in the dark.